Electric-field control of the magnetic anisotropy in an ultrathin (Ga,Mn)As/(Ga,Mn)(As,P) bilayer

T. Niazi,[1] M. Cormier,[1] D. Lucot,[1] L. Largeau,[1] V. Jeudy,[2,3] J. Cibert,[4] and A. Lemaître[1]

[1)] *Laboratoire de Photonique et de Nanostructures, CNRS, 91460 Marcoussis, France*

[2)] *Laboratoire de Physique des Solides, Université Paris-Sud – CNRS, 91405 Orsay, France*

[3)] *Université Cergy-Pontoise, 95000 Cergy-Pontoise, France.*

[4)] *Institut Néel, CNRS – Université Joseph Fourier, 38042 Grenoble, France*

(Dated: 30 November 2012)

We report on the electric control of the magnetic anisotropy in an ultrathin ferromagnetic (Ga,Mn)As/(Ga,Mn)(As,P) bilayer with competing in-plane and out-of-plane anisotropies. The carrier distribution and therefore the strength of the effective anisotropy is controlled by the gate voltage of a field effect device. Anomalous Hall Effect measurements confirm that a depletion of carriers in the upper (Ga,Mn)As layer results in the decrease of the in-plane anisotropy. The uniaxial anisotropy field is found to decrease by a factor ~ 4 over the explored gate-voltage range, so that the transition to an out-of-plane easy-axis configuration is almost reached.

The electric control of the magnetic state is a very attractive approach to bit-state manipulation in magnetic memories or logic devices. The first demonstrations in ferromagnetic semiconductors were reported in ultrathin layers of (In,Mn)As or (Ga,Mn)As.[1–3] In these compounds, the ferromagnetic phase is carrier-mediated. The carrier density is low enough to produce sizeable effects on the ferromagnetic properties by depleting or accumulating carriers in a field-effect device (FED). In the most recent studies, the electric control of the magnetic anisotropy has been demonstrated,[4–7] a first step toward reversible magnetization switching by electrical means.[8]

However, achieving a significant modification of the magnetic anisotropy by using its specific carrier-dependence[9] requires a large change of the carrier density.[10] Large depletion can be achieved in 4-7 nm thick (Ga,Mn)As layers.[3–5] However, as the depleted region expands over the whole ferromagnetic conductive channel, all its ferromagnetic properties are affected, which eventually leads to disappearance of the ferromagnetic order. Hence, it is an important issue to find alternative methods to extend the magnetic anisotropy tunability under electric field while preserving essential ferromagnetic parameters such as large Curie temperature and magnetization.

Here, we introduce and demonstrate a structure designed to enhance the electrical control of the magnetic anisotropy without resorting to excessively large depletion. This configuration eventually leads to the electric-field control of the in-plane and out-of-plane components of the magnetization.

Our structure relies on an ultrathin (Ga,Mn)As/(Ga,Mn)(As,P) bilayer embedded in a metal-insulator-semiconductor FED (Fig. 1a), grown on (001) GaAs. In this specific strain configuration, the [001] direction is an easy axis in (Ga,Mn)(As,P) and a hard axis in (Ga,Mn)As.[11] Therefore, the holes mediating ferromagnetism explore two magnetic regions with competing anisotropies. In our device, the bilayer thickness (4 nm) is smaller than the exchange length ($\sim$ 10 nm),[12] so that the magnetization should be homogeneous over the hole gas region. Therefore, the effective magnetic anisotropy results from the balance between the contributions of the two layers. Applying a gate voltage controls the depletion length, which affects mostly the layer closer to the gate oxide, (Ga,Mn)As in our case. This should in turn lower or increase the contribution of the (Ga,Mn)As layer to the bilayer magnetic anisotropy (see Fig. 1b).

The bilayer and the GaAs cap were grown at $\sim$ 220°C, the rest of the structure at

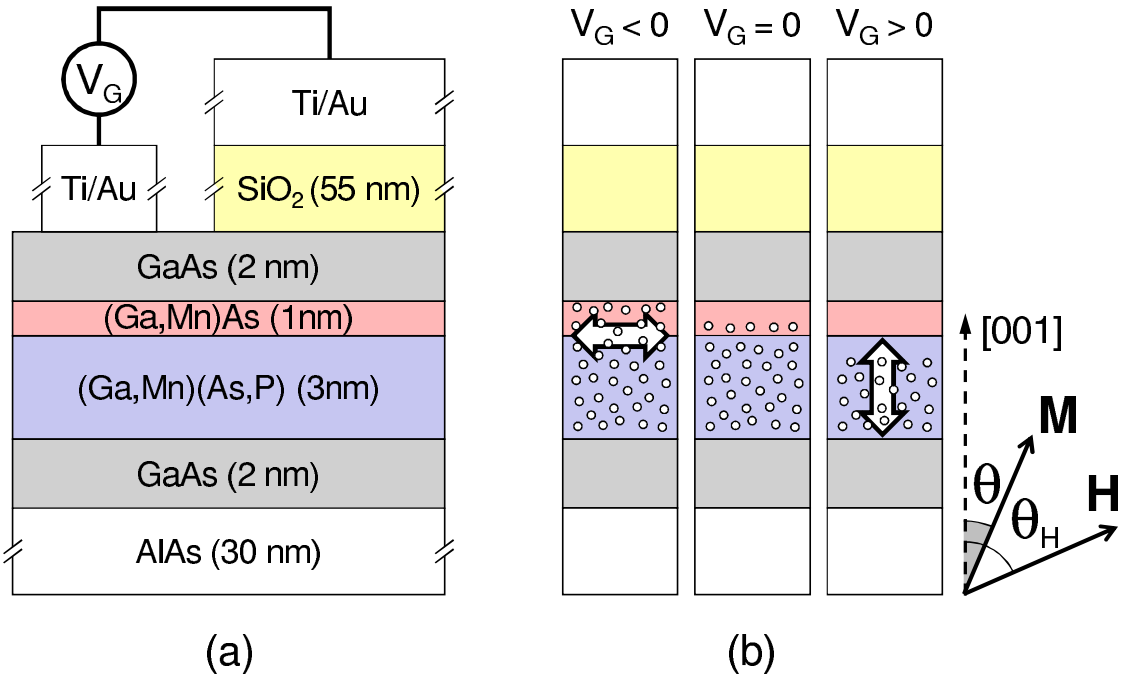

FIG. 1. (a) Schematic diagram of the bilayer structure embedded in a field-effect device. (b) A schematic drawing illustrating the principle of electric-field control of the bilayer easy axis (depicted by white arrows).

$\sim$ 550°C. The as-grown Mn and P concentrations, both around 10 %, were determined from calibration samples. The sample was annealed on a hot plate for 105 min at 200°C to decrease the amount of interstitial Mn ions, leading to an effective Mn moment concentration of about $\sim$ 5 % as measured on similar, but thicker samples.[13] Hall bars were processed by optical lithography and chemical etching. A 55 nm thick SiO_2 gate-oxide layer was deposited by plasma-enhanced chemical vapor deposition at 200°C. A Ti/Au film serving as the gate was then evaporated over the conductive channel. The structural quality was checked, after annealing, by high-resolution scanning transmission electron microscopy. The magnetic layers does not exhibit any extended defects such as MnAs or MnP aggregates. High-angle annular dark-field (HAADF) Z-contrasted images revealed the bilayer structure: the (Ga,Mn)(As,P) layer appeared darker than the (Ga,Mn)As layer, with a well defined interface. A thin layer ($\sim$ 2 nm) consisting of gallium and arsenic oxide was observed, corresponding to the oxidization of the protecting GaAs cap layer. Last, the SiO_2 layer appeared homogeneous, amorphous, showing no sign of crystallization, and stoichiometric as confirmed by energy-dispersive x-ray spectrometry.

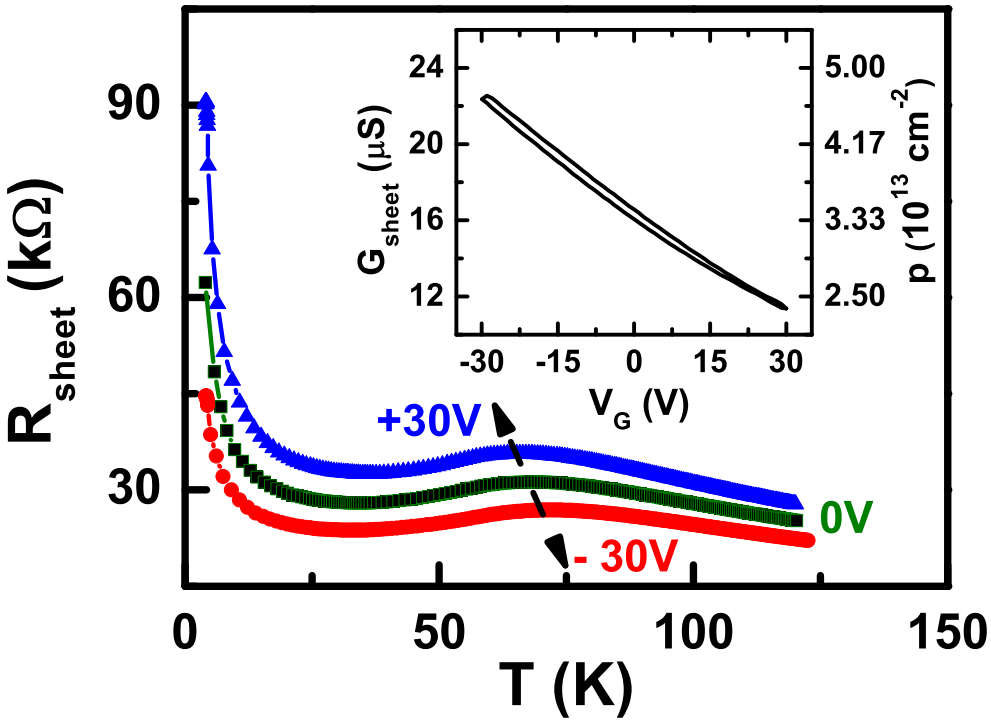

FIG. 2. Temperature-dependence of the sheet resistance for three values of the gate voltage, as indicated. Inset: sheet conductance *vs* V_G measured at 4.2 K and zero magnetic field; the right scale gives an estimate of the hole density.

Magneto-transport experiments were performed on Hall bars aligned along [110] (channel length 215 μm, width 40 μm), connected by Ti (20 nm)/Au (200 nm) metallic pads. The longitudinal and transverse resistivities were measured by a lock-in technique with high-impedance pre-amplifiers, keeping the current low (20 nA) so that the voltage drop across the Hall bar was negligible compared to the gate voltage. The gate voltage excursion was limited by the breakdown voltage to $V_G = \pm 30$ V (corresponding to an electric field of ± 5.5 MV.cm^{-1}).

The temperature-dependence of the sheet resistance $R_{\rm sheet}$ is shown in Fig. 2 for three values of the gate voltage ($V_G = 0, \pm 30$ V). Positive and negative voltages tend to achieve the hole gas depletions schematically described in Fig. 1(b). Below 30 K, the resistance increases, indicating that the system is on the insulator side close to the metal-insulator transition. At 4.2 K, the sheet conductance $G_{\rm sheet}$ varies by a factor 2 for $V_G = \pm 30$ V

(Fig. 2 inset). Hardly any hysteresis with electric field is observed, indicating the absence of carriers deeply trapped within the oxide layer or at the oxide–semiconductor interface. If we use the constant-mobility model of Ref. 4 and assume equal resistivities for both layers, we estimate a carrier density $p \sim 3.3 \times 10^{13}$ cm^{-2} at 0 V and a density change $\Delta p \sim 2.3 \times 10^{13}$ cm^{-2} between ± 30 V (assuming a SiO_2 dielectric constant of 3.9). With these assumptions, however, we probably overestimate Δp. Indeed, on the insulator side, close to the metal-insulator transition, we may expect the presence of weakly localized carriers, hardly contributing to the conductance, but fully contributing to ferromagnetism and fully affected by the electric field. Then, a better estimate of the carrier density would be closer to the $\sim$10% conductance variation measured at higher temperature.

The cusp around 60 K indicates the onset of the ferromagnetic phase. A better estimate of the Curie temperature T_C and its change ΔT_C with V_G can be inferred from the derivative of $R_{\rm sheet}$:[14] $T_C \sim 54$ K at $V_G = 0$ V and $\Delta T_C \sim 3$ K between ± 30 V, a moderate change, comparable with that of previous reports.[3–5]

We now turn to the study of the magnetic anisotropy, deduced from anomalous Hall effect (AHE) measurements. Magnetic hysteresis loops measured for $V_G = 0, \pm 30$ V are shown in Fig. 3 for two directions of the applied magnetic field, perpendicular to the sample (Fig. 3(a)) and at 45° towards $[1\bar{1}0]$ (Fig. 3(b)). For each V_G-value, the Hall resistance ($R_{\rm Hall}$) was normalized to its value ($R^s_{\rm Hall}$) measured at saturation with the field along [001] ($R^s_{\rm Hall} = 1.3$ kΩ at $V_G = 0$ V). In (Ga,Mn)As and for the explored magnetic-field range, $R_{\rm Hall}$ is dominated by the AHE: $R_{\rm AHE} = \frac{R_S}{t} M_\perp$, where R_S is the AHE coefficient, t the conducting layer thickness, and $M_\perp$ the perpendicular component of the magnetization. R_S usually depends on the magnetoresistance. However, magnetoresistance was found to be of the order of a few percent over the investigated magnetic-field range, sufficiently weak to consider that the field-dependence shown in Fig. 3 mostly reflects the variation of $M_\perp$. The small contribution of the planar Hall effect was also not taken into account.

The curves in Fig. 3(a) display a saturation above $|H| \sim 500$ Oe, and hysteresis below with a strong shape modification with V_G. In particular, $|R_{\rm Hall}/R^s_{\rm Hall}|$ at $H = 0$ Oe decreases when V_G is scanned from +30 V to −30 V, indicating a decrease of the remanent magnetization along [001]. As nucleation of magnetization reversal and domain-wall propagation contribute to the hysteresis-loop shape, we confirm the role of anisotropy by considering loops obtained with the field applied at 45° towards $[1\bar{1}0]$, [Fig. 3(b)], which contain a reversible contribution

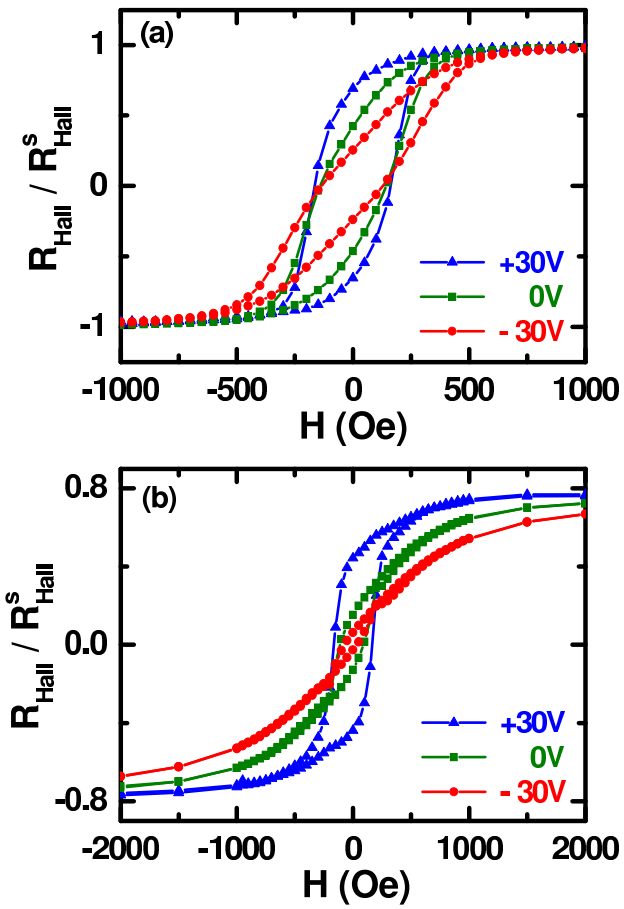

FIG. 3. Field-dependence of the Hall resistance for $V_G = 0, \pm 30$ V at 4.2 K. The field was applied along [001] (a), or tilted at 45° towards $[1\bar{1}0]$ (b). Each curve is normalized to the saturation value measured with the field along [001].

from coherent magnetization changes. During a field scan from 2000 to 500 Oe, $|R_{\rm Hall}/R^s_{\rm Hall}|$ decreases: this indicates that [001] is a hard axis. The decrease is larger for $V_G = -30$ V than for +30 V, thus confirming that a negative gate voltage reinforces the bilayer anisotropy in-plane character.

For a quantitative study, the applied field was rotated in the (110) plane by an angle θ_H from [001]. For a field (6000 Oe) much larger than the saturation field ($\sim$ 500 Oe), the Hall resistance exhibits a cosine-like variation (not shown): this is compatible with a constant magnetization aligned on the applied field, and R_S almost independent of θ. The angular dependence for a field value close to the saturation field is shown in Fig. 4(a). Clear deviations from the cosine law are observed, with sharper extrema around $\theta_H = 0$ and 180° ([001] and $[00\bar{1}]$ directions) at negative voltage. We model this below as a result of the

quasi-coherent magnetization rotation, with a competition between the applied magnetic field and the anisotropy.

The angular dependences measured at 500 and 1000 Oe, are fitted by minimizing the free energy given by:

$$F(\theta) = M.\left(-H\cos(\theta - \theta_H) + \frac{H_{\text{eff}}}{2}\cos^2\theta - \frac{H_{\text{cub}}}{4}\cos^4\theta\right) \quad (1)$$

where θ is the magnetization angle. H_{cub} describes the cubic anisotropy. H_{eff} includes the demagnetizing field and a combination of the magneto-crystalline, uniaxial, and cubic anisotropy fields.[15] Eq. 1 assumes that the magnetization remains in the (110) plane. This is likely since we find $H_{\text{cub}} < |H|$; moreover an additional anisotropy within the (001) plane exists in (Ga,Mn)As which usually favors the $[1\bar{1}0]$ orientation.[13] Figure 4(a) shows the good fit quality.

Figure 4(b) shows the anisotropy fields extracted from the fits, as a function of the gate voltage. H_{cub} is found to vary weakly with V_G, keeping a value ($\sim$ 300 Oe) comparable to those reported in Ref. 13 for similar Mn concentrations. We observe a strong variation of H_{eff}. For each set of the anisotropy field values, the overall bilayer anisotropy can be understood from the free-energy landscape at $H = 0$ (Eq. 1). For $V_G < 0$ and up to ~ 7 V, $H_{\text{eff}} > H_{\text{cub}}$, so that there is a single free-energy minimum, corresponding to an easy axis in the (001) plane. For $V_G \sim 7$ V, $H_{\text{eff}} = H_{\text{cub}}$, hence a second minimum appears corresponding to the [001] direction. At $V_G = 30$ V, $H_{\text{eff}}/H_{\text{cub}} \sim 1/2$, hence we reach the point where both minima are equivalent. By extrapolating the data in Fig. 4(b), a single free-energy minimum corresponding to an easy axis along the [001] direction would be obtained at $V_G \sim 50$ V. Over such a voltage excursion, the magnetic easy axis could be tuned from in-plane to out-of-plane, achieving the magnetic configuration depicted in Fig. 1(b).

Our results are consistent with an electric control of the competition between the opposite uniaxial anisotropies of each layer [Fig. 1(b)]. At 0 V, the bilayer has a moderate in-plane anisotropy, showing that the topmost (Ga,Mn)As layer is not totally depleted by transfer to the hole traps at the interface with SiO_2.[4,6] This suggests a rather moderate trap density. We cannot also exclude a carrier transfer from the (Ga,Mn)(As,P) layer toward the (Ga,Mn)As layer, as P substitution induces a valence-band offset between the two magnetic layers. At -30 V, the depletion length is reduced, the hole gas now extends more into the (Ga,Mn)As layer, and the in-plane anisotropy is reinforced. At +30 V, depletion reduces the contribution

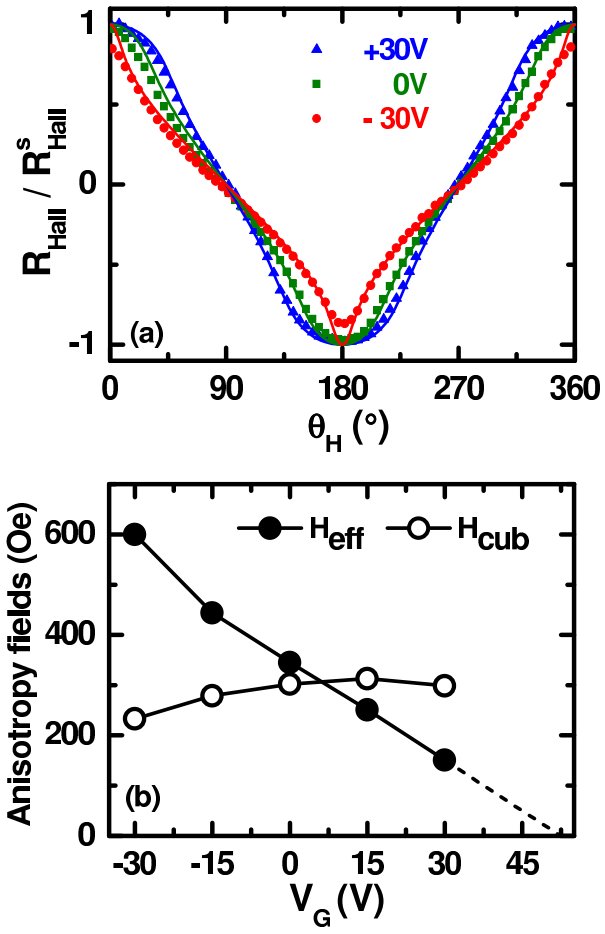

FIG. 4. (a) Angular dependence of the Hall resistance for a 500 Oe field (symbols: experiment; lines: fits with the model described in text). (b) Dependence of the anisotropy fields on the gate voltage, extracted from the fits at 500 and 1000 Oe.

from the (Ga,Mn)As layer, enhancing the relative contribution of the (Ga,Mn)(As,P) layer to the bilayer anisotropy. The fact that we did not reach an out-of-plane easy-axis at +30 V suggests that the depletion induced by the gate is rather weak, smaller that what is suggested by the constant-mobility model applied down to low temperature.

Other origins for this electrical tuning of the anisotropy can be ruled out. Although the gate voltage is expected to shift the boundary between the hole gas and the depleted region, as schematized in Fig. 1, this boundary is not totally abrupt, and a variation of the 3D carrier density is expected, at least when approaching total depletion of the channel. This mechanism has been used to electrically control the Curie temperature or the cubic anisotropy.[4–7] In the present case, these two parameters vary only very weakly with the gate

voltage, so that we can rule out such a mechanism for the variation of H_{eff}. A weakening of the contribution from the demagnetizing effect is also not likely, since we worked far below the Curie temperature.

In conclusion, clear modifications of the magnetic anisotropy have been achieved in an ultrathin (Ga,Mn)As/(Ga,Mn)(As,P) stack upon applying electric field. We attribute this effect to the electric control of the competition between the in-plane and out-of-plane anisotropies of both layers. While in this study, large electric fields were needed to observe sizeable modifications, switching to high-k gate oxides, such as HfO_2, should allow a better control of the bilayer magnetic anisotropy with lower values of the gate voltage.

The work was performed in the framework of the ANR MANGAS project (2010-BLANC-0424).

REFERENCES

[1]H. Ohno, D. Chiba, F. Matsukura, T. Omiya, E. Abe, T. Dietl, Y. Ohno, and K. Ohtani, Nature **408**, 944 (2000).

[2]D. Chiba, M. Yamanouchi, F. Matsukura, and H. Ohno, Science **301**, 943 (2003).

[3]I. Stolichnov, S. W. E. Riester, H. J. Trodahl, N. Setter, A. W. Rushforth, K. W. Edmonds, R. P. Campion, C. T. Foxon, B. L. Gallagher, and T. Jungwirth, Nature Mater. **7**, 464 (2008).

[4]D. Chiba, M. Sawicki, Y. Nishitani, Y. Nakatani, F. Matsukura, and H. Ohno, Nature **455**, 515 (2008).

[5]M. H. S. Owen, J. Wunderlich, V. Novák, K. Olejník, J. Zemen, K. Výborný, S. Ogawa, A. C. Irvine, A. J. Ferguson, H. Sirringhaus, and T. Jungwirth, New J. Phys. **11**, 023008 (2009).

[6]M. Sawicki, D. Chiba, A. Korbecka, Y. Nishitani, J. A. Majewski, F. Matsukura, T. Dietl, and H. Ohno, Nat. Phys. **6**, 22 (2010).

[7]E. Mikheev, I. Stolichnov, Z. Huang, A. W. Rushforth, J. A. Haigh, R. P. Campion, K. W. Edmonds, B. L. Gallagher, and N. Setter, Appl. Phys. Lett. **100**, 262906 (2012).

[8]D. Chiba, Y. Nakatani, F. Matsukura, and H. Ohno, Appl. Phys. Lett. **96**, 192506 (2010).

[9]T. Dietl, H. Ohno, and F. Matsukura, Phys. Rev. B **63**, 195205 (2001).

[10]L. Thevenard, L. Largeau, O. Mauguin, A. Lemaître, K. Khazen, and H. J. von

Bardeleben, Phys. Rev. B **75**, 195218 (2007).

[11]A. Lemaître, A. Miard, L. Travers, O. Mauguin, L. Largeau, C. Gourdon, V. Jeudy, M. Tran, and J.-M. George, Appl. Phys. Lett. **93**, 021123 (2008).

[12]S. Haghgoo, M. Cubukcu, H. J. von Bardeleben, L. Thevenard, A. Lemaître, and C. Gourdon, Phys. Rev. B **82**, 041301 (2010).

[13]M. Cubukcu, H. J. von Bardeleben, K. Khazen, J. L. Cantin, O. Mauguin, L. Largeau, and A. Lemaître, Phys. Rev. B **81**, 041202 (2010).

[14]V. Novák, K. Olejník, J. Wunderlich, M. Cukr, K. Výborný, A. W. Rushforth, K. W. Edmonds, R. P. Campion, B. L. Gallagher, J. Sinova, and T. Jungwirth, Phys. Rev. Lett. **101**, 077201 (2008).

[15]X. Liu, Y. Sasaki, and J. K. Furdyna, Phys. Rev. B **67**, 205204 (2003).